Supplementary Material

In situ electropolymerizable thiophene-diketopyrrolopyrrole-based organic cathode for efficient lithium-organic batteries†

Experimental

Materials: All reagents were obtained from commercial sources and used without further purification. Th-DPP was purchased from SunaTech (Suzhou, China) and Super P Li (SP) was purchased from Canrd Technology Co., Ltd. Polyvinylene difluoride (PVDF, Mw ~1,000,000) was purchased from Beijing Huawei Ruike Chemical Co., Ltd. The components of the electrolyte, including Lithium hexafluorophosphate (1.0M $LiPF_6$ in EC:DMC = 1:1 Vol%) were purchased from DoDoChem.

Characterization: Cyclic voltammetry (CV) and electrochemical impedance spectroscopy (EIS) measurements were performed on an electrochemical workstation (CHI660E). CV electropolymerization was performed with a three-electrode system with ITO/PET as the work electrode, Ag/AgCl as the reference electrode, a platinum wire as the counter electrode, and Bu_4NPF_6 (0.1 M) in dichloromethane as the electrolyte. FTIR spectra data were collected with a Nicolet iS50 Fourier transform infrared spectrometer or a Bruker Alpha II FTIR spectrometer in the 400–4000 cm^{-1} region with an ATR model. The electronic structures of the molecules were studied by Density Functional Theory (DFT) calculations performed at the B3LYP/6-31G(d,p) level to illustrate the frontier molecular orbitals and energy levels of Th-DPP and its 2–4 repeat unit oligomers using the Gaussian 09 package40.[S1] Galvanostatic charge/discharge curves and rate capability tests were carried out on a Land test system (CT3001A, China). Scanning electron microscopy (SEM) characterization and energy dispersive spectroscopy (EDS) mappings were conducted using a Hitachi SU8200 instrument. UV-vis spectra were recorded on a SIMADZU UV-3600i Plus spectrophotometer. Thermogravimetry (TG) measurements were performed on a SDT Q500 (TA Instruments) under a N_2 atmosphere.

Cathode fabrication, coin cell assembly, and battery test: The conventional organic electrode is composed of a mixture of 30 wt% electroactive materials (Th-DPP), 60 wt% Super P Li (SP), and 10 wt% binder (PVDF). The mixing process was conducted using a conventional mortar and pestle, during which

Th-DPP, SP, and PVDF were added to the mortar in sequence and ground for 15 min. The mixture was poured into a tablet mold and punched into circular sheets with 12 mm in diameter. The areal mass loading for each electrode was approximately 4.5–5.5 mg cm^{-2}, and the capacity was calculated based on the mass of active material of each electrode. The electrodes were dried at 80 °C in a vacuum oven for over 8 h before assembling coin-type cells in an argon-filled glovebox. The coin cells were composed of such electrodes as the cathode, lithium metal disc as the anode, glass fiber (GF) as the separator and 1.0 M $LiPF_6$ dissolved in EC-DMC (1:1, v:v) as the electrolyte.

Three electrodes with other weight contents (40 wt%, 50 wt%, and 60 wt%) of Th-DPP were prepared. The corresponding electrode Th-DPP/SP/PVDF component ratios were 40/50/10, 50/40/10, and 60/30/10 in wt%. The remaining fabrication, coin cell assembly, and battery test were similar to those of the conventional 30 wt% Th-DPP-based battery mentioned above.

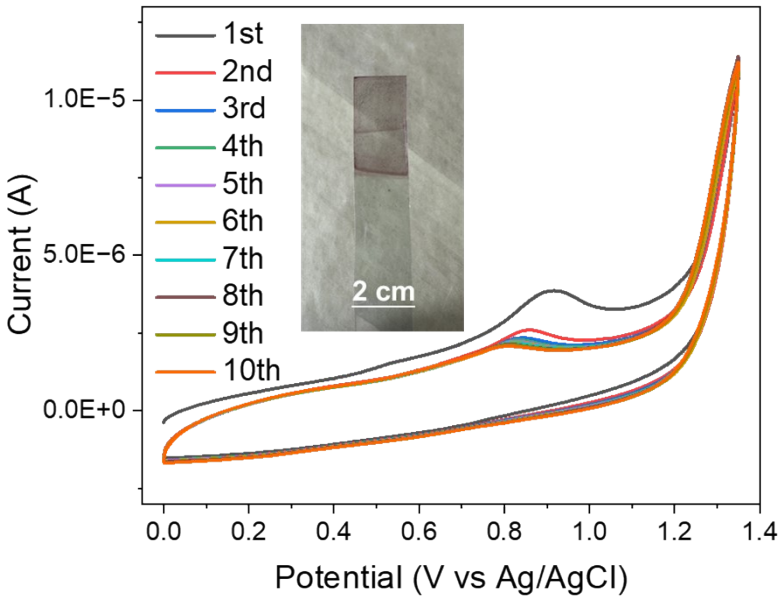

Fig. S1. CV curves of Th-DPP solution at potential range of 0–1.35 V, inset is the digital photograph of Th-DPP electropolymerized on ITO/PET.

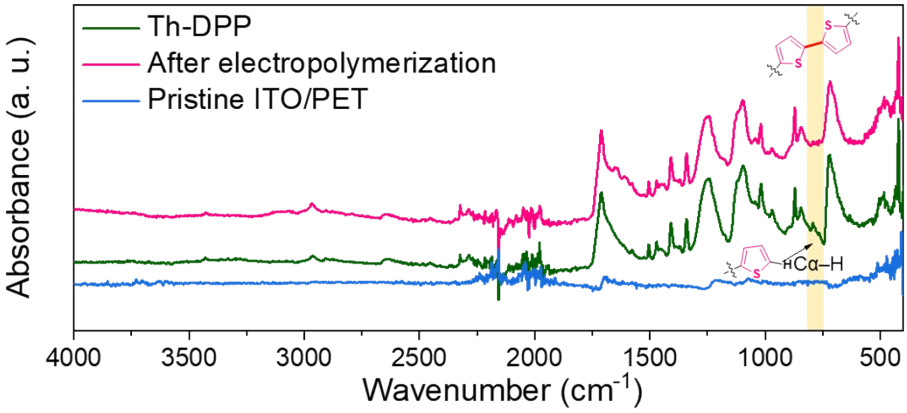

Fig. S2. FTIR spectra of Th-DPP before and after electropolymerization and the pristine ITO/PET substrate.

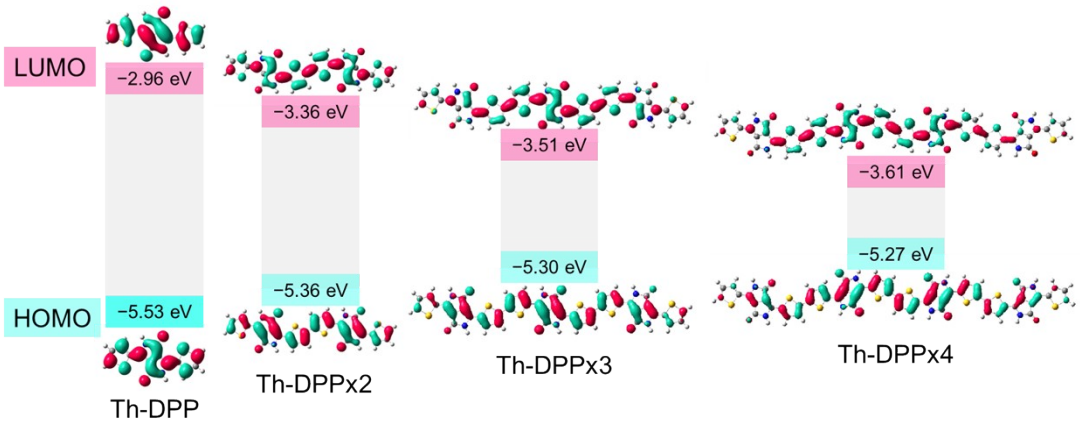

Fig. S3. Frontier molecular orbitals of Th-DPP and its 2–4 repeat unit oligomers obtained from DFT calculations.

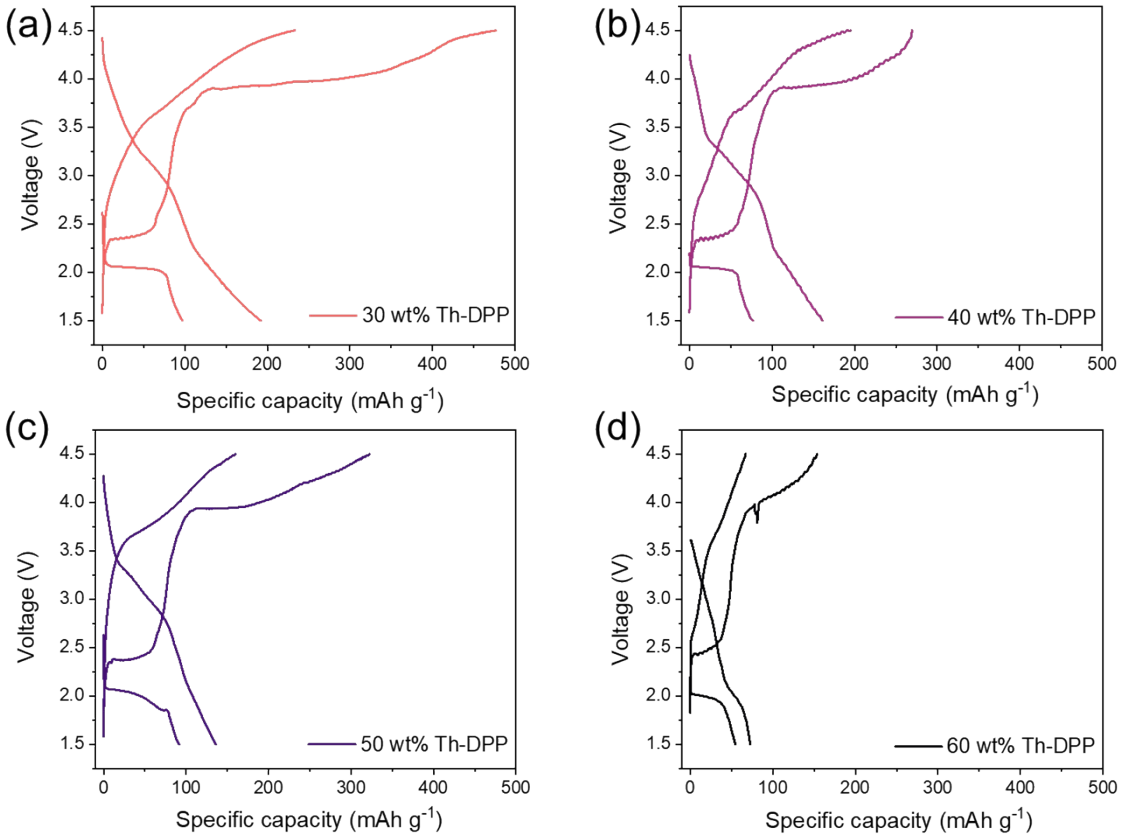

Fig. S4. The first two cycles of discharge/charge plots of Th-DPP cathodes with different weight contents of Th-DPP.

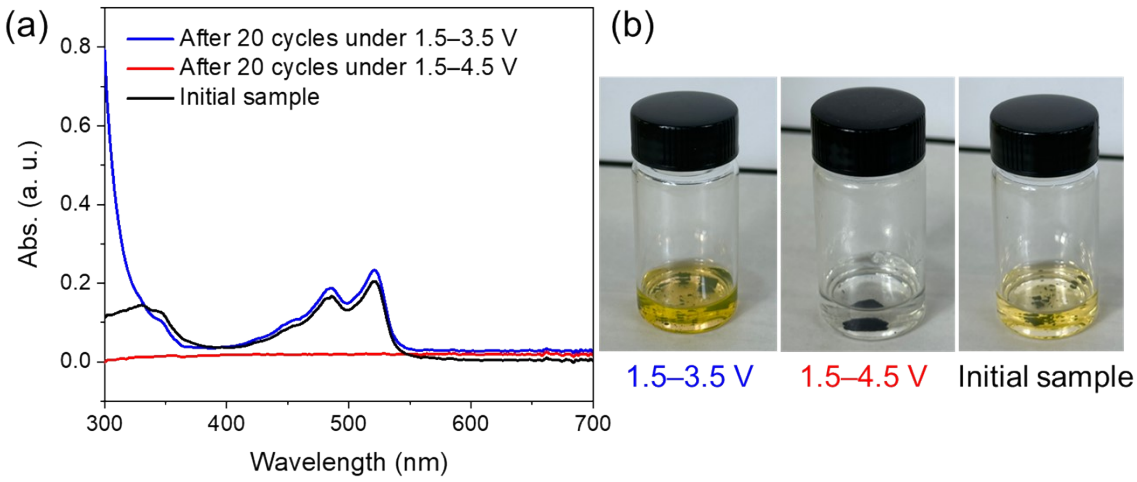

Fig. S5. (a) UV-vis spectra of Th-DPP cathodes in DMC solutions. (b) Images of Th-DPP cathodes soaked in DMC solutions.

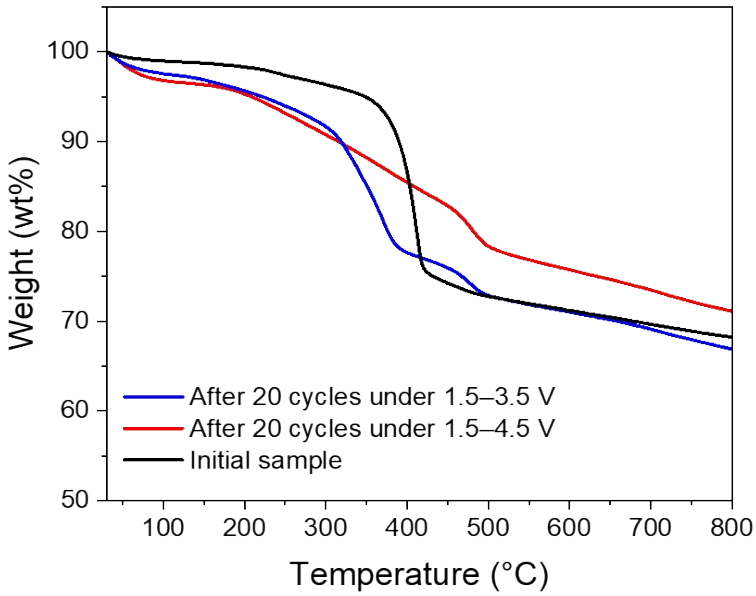

Fig. S6. TG curves of Th-DPP cathodes.

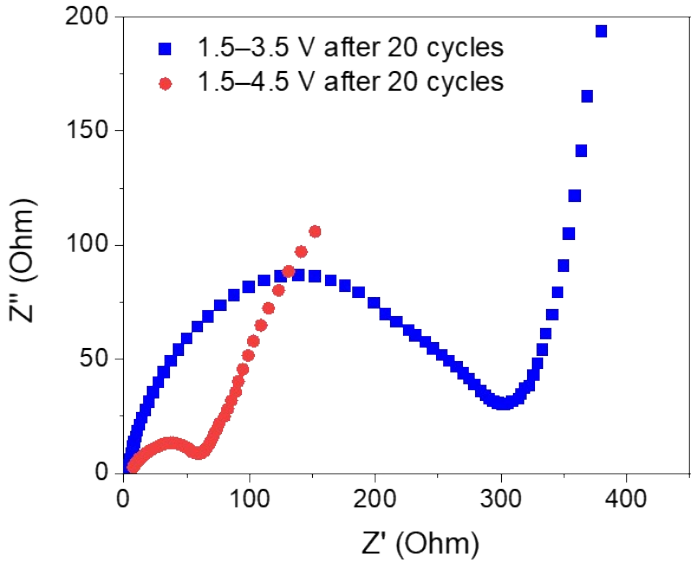

Fig. S7. Nyquist plots of Th-DPP cathodes.

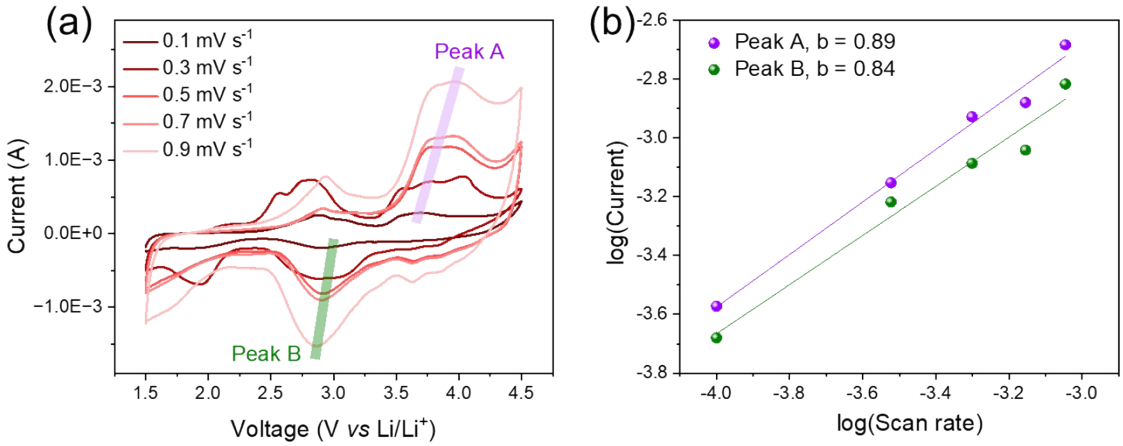

Fig. S8. (a) CV curves and (b) the *b*-value analysis of the batteries at different scan rates.

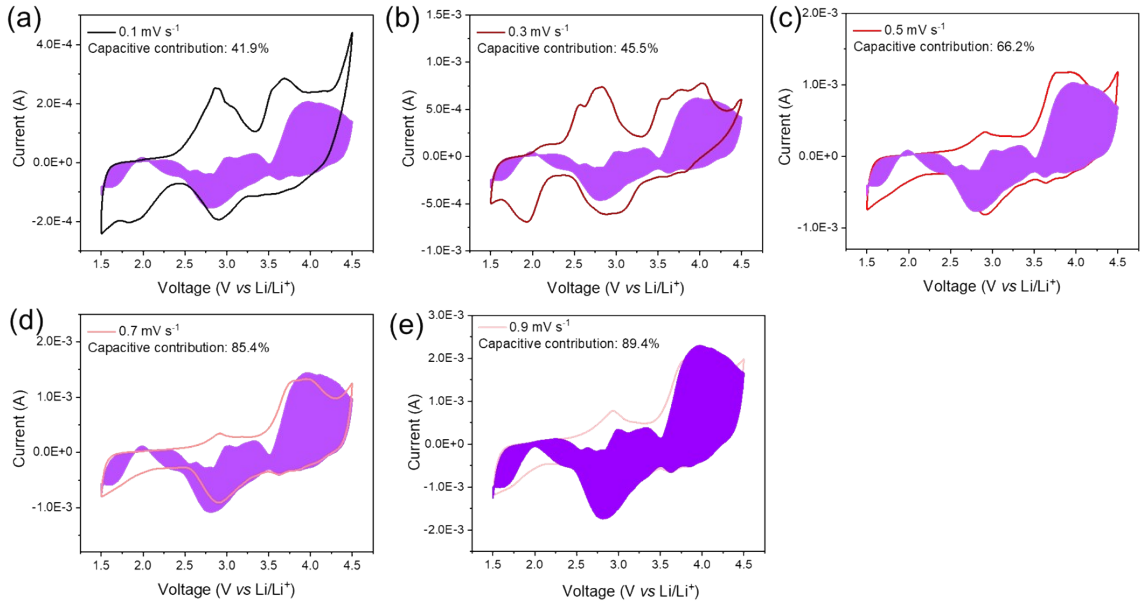

Fig. S9. CV curves and capacitive contributions of Th-DPP cathodes at scan rates of (a) 0.1, (b) 0.3, (c) 0.5, (d) 0.7, and (e) 0.9 mV s^{-1}.

References:

[S1]M. J. Frisch, G. W. Trucks, H. B. Schlegel, G. E. Scuseria, M. A. Robb, J. R. Cheeseman, G. Scalmani, V. Barone, B. Mennucci, G. A. Petersson, H. Nakatsuji, M. Caricato, X. Li, H. P. Hratchian, A. F. Izmaylov, J. Bloino, G. Zheng, J. L. Sonnenberg, M. Hada, M. Ehara, K. Toyota, R. Fukuda, J. Hasegawa, M. Ishida, T. Nakajima, Y. Honda, O. Kitao, H. Nakai, T. Vreven, J. A. Montgomery Jr, J. E. Peralta, F. Ogliaro, M. Bearpark, J. J. Heyd, E. Brothers, K. N. Kudin, V. N. Staroverov, R. Kobayashi, J. Normand, K. Raghavachari, A. Rendell, J. C. Burant, S. S. Iyengar, J. Tomasi, M. Cossi, N. Rega, J. M.

Millam, M. Klene, J. E. Knox, J. B. Cross, V. Bakken, C. Adamo, J. Jaramillo, R. Gomperts, R. E. Stratmann, O. Yazyev, A. J. Austin, R. Cammi, C. Pomelli, J. W. Ochterski, R. L. Martin, K. Morokuma, V. G. Zakrzewski, G. A. Voth, P. Salvador, J. J. Dannenberg, S. Dapprich, A. D. Daniels, O. Farkas, J. B. Foresman, J. V. Ortiz, J. Cioslowski and D. J. Fox, Gaussian 09, Revision A.02, Gaussian, Inc., Wallingford CT, 2009.